

A Photometric Analysis of ZZ Ceti Stars: A Parameter-Free Temperature Indicator?

P Bergeron¹, S K Leggett² and H C Harris³

¹ Département de Physique, Université de Montréal, C.P. 6128, Succ. Centre-Ville, Montréal, Québec H3C 3J7, Canada

² Gemini Observatory, Northern Operations Center, 670 North A'ohoku Place, Hilo, Hawaii 96720, USA

³ US Naval Observatory, Flagstaff Station, Flagstaff, Arizona 86001, USA

E-mail: bergeron@astro.umontreal.ca, sleggett@gemini.edu, hch@nofs.navy.mil

Abstract. We present a model atmosphere analysis of optical *VRI* and infrared *JHK* photometric data of about two dozen ZZ Ceti stars. We first show from a theoretical point of view that the resulting energy distributions are not particularly sensitive to surface gravity or to the assumed convective efficiency, a result which suggests a parameter-free effective temperature indicator for ZZ Ceti stars. We then fit the observed energy distributions with our grid of model atmospheres and compare the photometric effective temperatures with the spectroscopic values obtained from fits to the hydrogen line profiles. Our results are finally discussed in the context of the determination of the empirical boundaries of the ZZ Ceti instability strip.

1. Introduction

The atmospheres of hydrogen-line (DA) white dwarfs become convective below roughly $T_{\text{eff}} \sim 17,000$ K, although it is only when they have cooled below $\sim 12,000$ K that a significant fraction of the total flux is transported by convection. At that point, the bottom of the convection zone sinks deeper into the star until it reaches a maximum depth of $\Delta M/M_{\star} \sim 10^{-6}$ near $T_{\text{eff}} \sim 5000$ K. Below 9000 K or so, convection in hydrogen-atmosphere white dwarfs becomes adiabatic, and the thermodynamic stratification is then specified by the value of the adiabatic gradient and the hydrostatic equilibrium equation. As such, the convective flux becomes almost completely independent of the assumed convective efficiency. Above that temperature, however, the structure of the atmosphere and the deeper stellar envelope depend sensitively on the way convection is treated in the model calculations. For instance, Bergeron et al. (1992) have shown that in the range $T_{\text{eff}} = 10,000 - 14,000$ K, the predicted energy distributions and line profiles are strongly affected by the parameterization of the mixing-length theory, the most commonly used formalism that can take into account convective energy transport in model atmosphere calculations.

This is unfortunately the precise range of effective temperature where the DA white dwarf pulsators, or ZZ Ceti stars, are found. According to the spectroscopic analysis of Gianninas et al. (2006, see also these proceedings), ZZ Ceti stars occupy a trapezoidal region in the $T_{\text{eff}} - \log g$ plane, with an empirical blue edge around 12,400 K and a red edge near 11,000 K, although both edges show a strong dependence on surface gravity. It must be stressed, however, that the atmospheric parameter determinations of ZZ Ceti stars depend strongly on the assumed

convective efficiency in the model atmosphere calculations. Moreover, this efficiency cannot be easily estimated from first principles. To overcome this situation, Bergeron et al. (1995) have attempted to calibrate the convective efficiency in the atmospheres of DA stars by comparing effective temperatures obtained from fits to Balmer line profiles with those derived from UV energy distributions. The authors convincingly demonstrate that the so-called $ML2/\alpha = 0.6$ parametrization of the mixing-length theory provides the best internal consistency between optical and UV effective temperatures, as well as trigonometric parallaxes, V magnitudes, and gravitational redshifts. This has been the parametrization used in all model atmosphere calculations since then.

In this paper, we present an independent method for estimating the internal consistency of this parametrization by fitting optical VRI and infrared JHK photometric energy distributions of ZZ Ceti stars with detailed model atmosphere calculations. In particular, we show that this technique provides a temperature indicator for ZZ Ceti stars that is independent of the assumed convective efficiency.

2. A Parameter-Free Temperature Indicator

Our fitting technique relies on the approach originally developed by Bergeron et al. (1997) in their study of cool white dwarfs. Briefly, the atmospheric parameters for each star are obtained by converting the optical and infrared photometry into observed fluxes, and by comparing the resulting spectral energy distributions with those predicted from model atmosphere calculations. The first step is accomplished by transforming the magnitudes into average stellar fluxes f_λ^m received at Earth using the calibration of Holberg et al. (2006). The observed and model fluxes, which depend on T_{eff} and $\log g$, are related by the equation $f_\lambda^m = 4\pi (R/D)^2 H_\lambda^m$ where R/D is the ratio of the radius of the star to its distance from Earth, and H_λ^m is the Eddington flux, properly averaged over the corresponding filter bandpass. We finally minimize the difference between observed and predicted fluxes at all bandpasses using our standard Levenberg-Marquardt minimization procedure. Only T_{eff} and the solid angle $\pi (R/D)^2$ are considered free parameters.

As a theoretical exploration of our method, we show in Figure 1 the predictions from our model atmospheres for various values of T_{eff} , $\log g$, and convective efficiency. Monochromatic Eddington fluxes are shown together with the average over the optical $UBVRI$ and infrared JHK filter bandpasses. One can already notice that if the U filter, and to a lesser extent, the B filter are omitted from the fits, the predicted energy distributions (normalized at V) do not depend on the assumed value of $\log g$ (middle panel), and more interestingly, they do not depend on the assumed parametrization of the mixing-length theory either (top panel; the ML1, ML2, and ML3 prescriptions are described in detail in Bergeron et al. 1995). Fortunately, the energy distributions remain sensitive to variations of effective temperature (bottom panel). Hence, by restricting our analysis to optical VRI and infrared JHK photometry, we obtain an *independent temperature scale* for ZZ Ceti stars that does not depend on the assumed value of $\log g$ (or mass) or convective efficiency.

3. Observational data

Since 2001, we have been obtaining time-averaged optical and infrared photometric observations of ZZ Ceti stars. Our data for 24 ZZ Ceti white dwarfs are summarized in Table 1. The optical photometry were secured with a CCD detector attached to the 1.0 m R/C reflector at the U.S. Naval Observatory in Flagstaff. Data were calibrated by observing standards from Landolt (1992) throughout each night and determining nightly extinction and color terms. When possible, stars were observed on two to three different nights to average out their variability. We measured the V magnitude for all 24 objects in our sample, and R and I magnitudes for only 9 and 20 objects, respectively. The infrared JHK photometry was secured for 19 objects

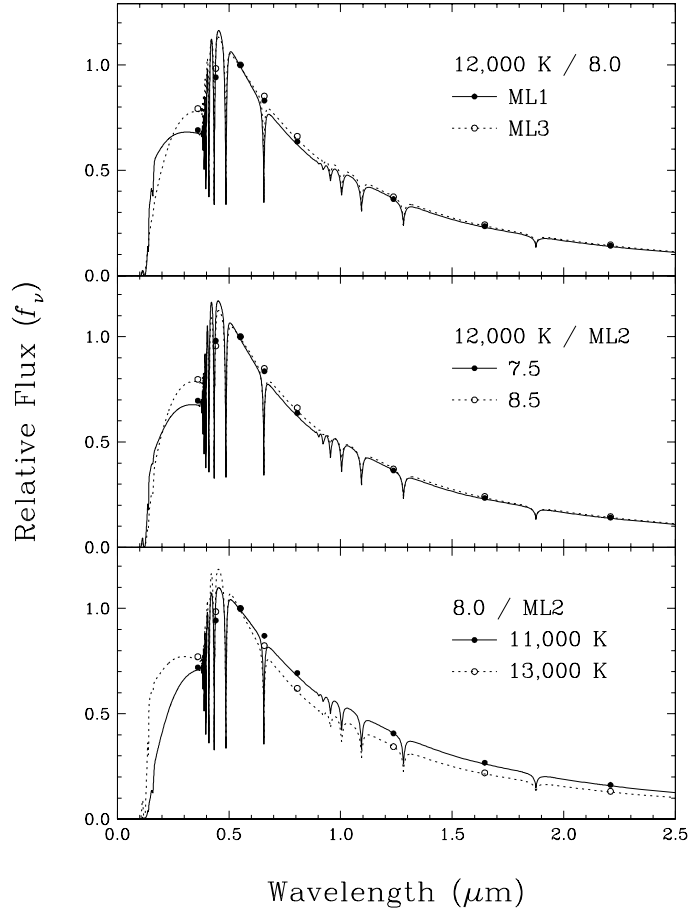


Figure 1. Energy distributions for white dwarfs in the ZZ Ceti temperature range for various values of T_{eff} , $\log g$, and convective efficiency. Also shown (open and filled circles) are the integrated fluxes over the optical $UBVR$ and infrared JHK filter bandpasses. All distributions are normalized at V .

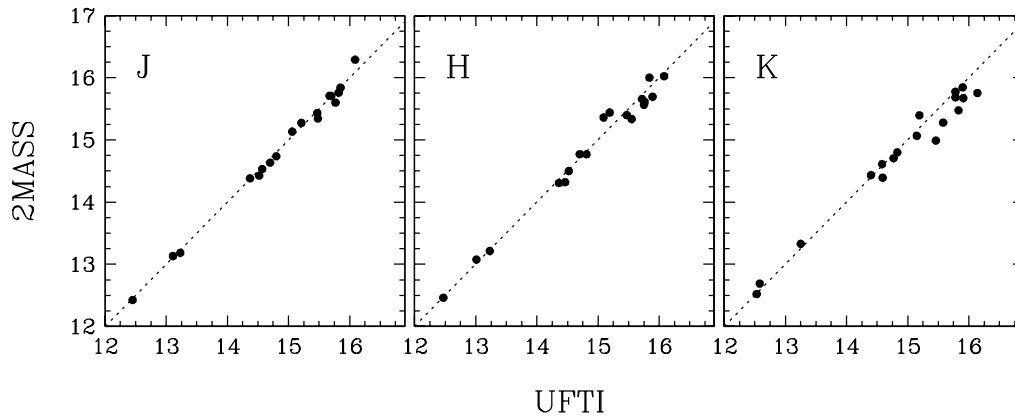


Figure 2. Comparison of infrared photometry for 17 ZZ Ceti stars in our sample that have both UFTI and 2MASS JHK measurements.

Table 1. Optical and infrared photometry of ZZ Ceti stars.

Name	V	R	I	J	UFTI		J	2MASS	
					H	K		H	K
Ross 548	14.16			14.37	14.36	14.40	14.38	14.30	14.43
KUV 02464+3239	16.03		16.03				15.97	15.92	15.44
HL 76	14.99		15.05	15.06	15.09	15.15	15.13	15.36	15.06
G38-29	15.59			15.70	15.75	15.78	15.70	15.56	15.77
HS 0507+0435B	15.33		15.39	15.47	15.55	15.58	15.43	15.33	15.27
GD 66	15.55		15.61	15.67	15.72	15.78	15.70	15.65	15.68
KUV 08368+4026	15.60	15.62	15.64	15.85	15.89	15.90	15.84	15.69	15.84
GD 99	14.51	14.53	14.52	14.70	14.70	14.77	14.63	14.77	14.70
G117-B15A	15.46	15.51	15.51	15.77	15.76	15.83	15.59	15.61	15.47
KUV 11370+4222	16.55	16.57	16.56	16.78	16.76	16.68			
G255-2	15.97	15.95	16.00				16.00	15.87	16.28
GD 154	15.26	15.24	15.29	15.48	15.47	15.46	15.34	15.39	14.98
G238-53	15.46	15.52	15.52				15.68	15.41	15.30
EC 14012-1446	15.66	15.66	15.69	15.82	15.84	15.91	15.75	16.00	15.67
GD 165	14.27	14.33	14.34	14.57	14.52	14.58	14.53	14.49	14.61
PG 1541+651	15.54		15.58				15.60	15.91	15.42
G226-29	12.24			12.45	12.47	12.53	12.42	12.46	12.52
G207-9	14.61		14.63	14.80	14.81	14.83	14.73	14.76	14.79
G185-32	12.98			13.23	13.23	13.25	13.18	13.21	13.32
GD 385	15.10		15.12	15.21	15.19	15.19	15.27	15.44	15.39
G232-38	16.83		16.79				16.34	15.97	16.01
PG 2303+243	15.26		15.34				15.49	15.41	15.70
G29-38	13.04		13.01	13.11	13.01	12.58	13.13	13.07	12.68
G30-20	16.07		16.04	16.09	16.08	16.14	16.29	16.02	15.75

using the U.K. Infrared Telescope (UKIRT) Fast-Track Imager (UFTI, Roche et al. 2003). The camera’s filters are on the Mauna Kea Observatories photometric system (Tokunaga et al. 2002), and the data were calibrated using standards from Leggett et al. (2006). Since the beginning of our survey, 2MASS photometry has also become available for 23 objects in our sample, and this data is reported in Table 1 and included in our analysis below. The UFTI and 2MASS *JHK* photometric observations for the 17 objects in common are compared in Figure 2. Both data sets agree extremely well, with the exception perhaps of the *K* filter for faint stars where our UFTI photometry is arguably better.

4. Photometric analysis

As discussed above, the magnitudes from Table 1 are converted into average fluxes using the appropriate filter transmission functions for each photometric system. Similarly, the model monochromatic fluxes are also averaged over the same filter sets. The model atmospheres used in this analysis are slightly different from those used by Bergeron et al. (1995) and in all previous analyses of ZZ Ceti stars by the Montreal group (Gianninas et al. 2006 and references therein). We are now making use of the extensive Stark broadening profiles calculated by Lemke (1997), while our earlier calculations relied on similar calculations by Schöning & Butler (1991, private communication) but for temperatures and densities characteristic of hot subdwarfs stars, which

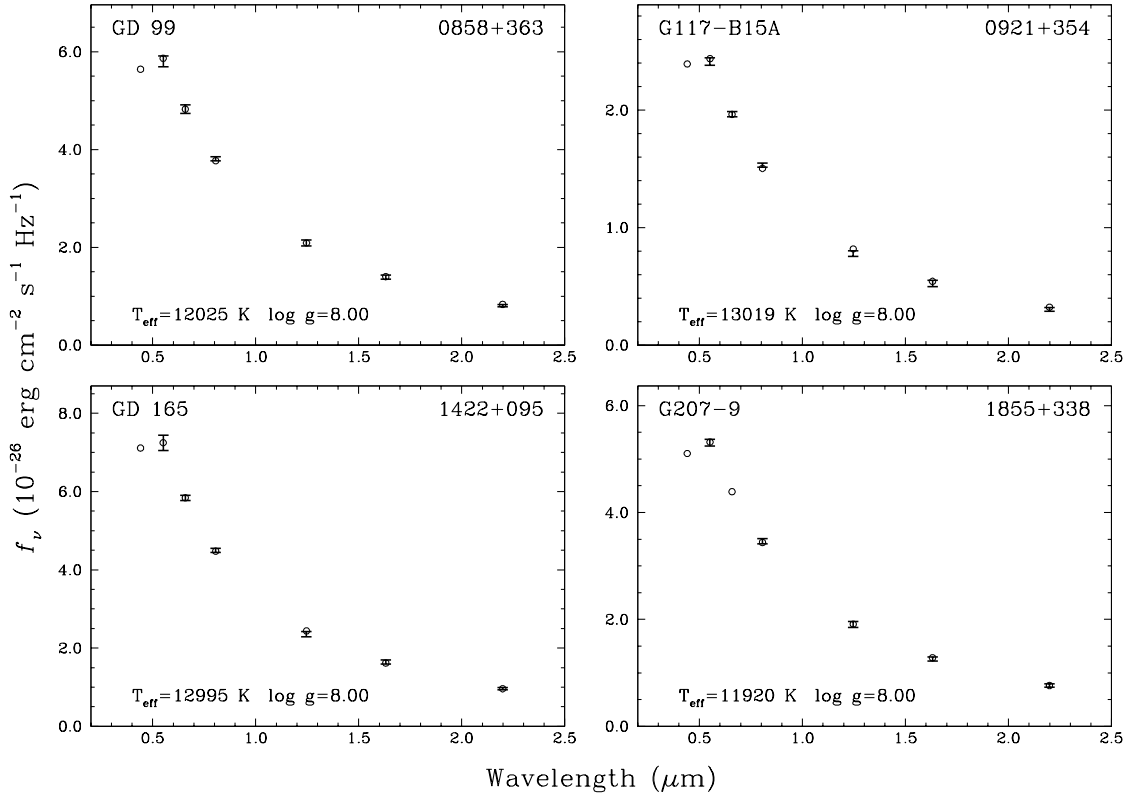


Figure 3. Sample fits to the energy distributions of ZZ Ceti stars. The *VRI* and *JHK* photometric observations are represented by error bars while the model fluxes are shown as open circles.

often required extrapolations in the higher density regime of white dwarf atmospheres. With these new models in hand, we redid the analysis of Bergeron et al. (1995) and found that a slightly more efficient version of the mixing-length theory, namely ML2 with $\alpha = 0.7$ (instead of 0.6), provides the best internal consistency between effective temperatures obtained from optical and UV spectra. Sample fits to the *VRI* and *JHK* energy distributions of four ZZ Ceti stars in our sample using these models are displayed in Figure 3. We assume in this figure a value of $\log g = 8.0$ for all objects.

The photometric effective temperatures for all ZZ Ceti stars in our sample are compared in Figure 4 with spectroscopic temperatures obtained from fits to the hydrogen Balmer lines using the so-called spectroscopic technique (see Bergeron et al. 1995 and references therein); the optical spectra are taken from the analysis of Gianninas et al. (2006). Both infrared data sets (UFTI and 2MASS) are considered independently in Figure 4. We also assume for our photometric fits a value of $\log g = 8.1$ for all objects, which corresponds to the average spectroscopic value of our sample ($\langle \log g \rangle = 8.143$, $\sigma = 0.166$). A variation of $\log g$ by ± 0.25 dex from the mean value changes the photometric temperatures by only 200 K, on average, as expected from the results displayed in the middle panel of Figure 1. Overall, the agreement observed in Figure 4 is satisfactory, although there are some objects with photometric temperatures significantly larger than the spectroscopic estimates. For these stars, however, we also notice that the photometric uncertainties appear larger. The object all the way to the left in the 2MASS panel is G29-

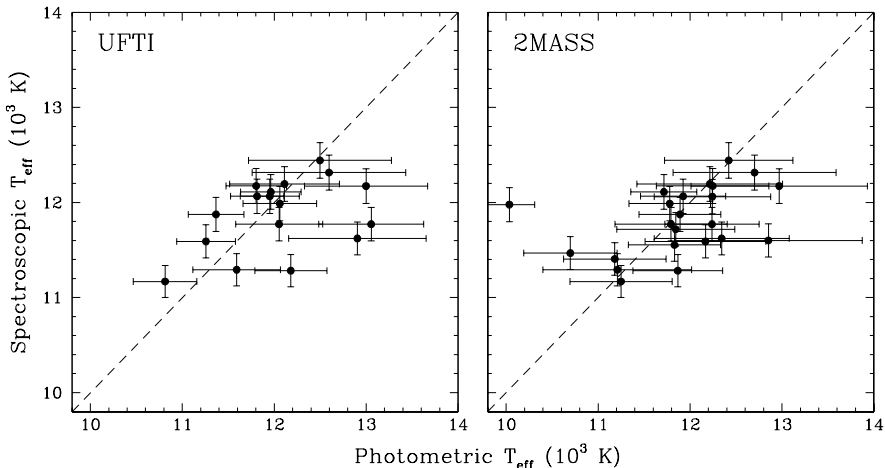


Figure 4. Comparison of photometric and spectroscopic effective temperatures for the two sets of infrared photometry used in our analysis. Model atmospheres calculated with the $ML2/\alpha = 0.7$ version of the mixing-length theory are used to obtain both estimates of T_{eff} .

38, a ZZ Ceti star with an infrared excess due to the presence of a dust disk, which affects our photometric temperature determination (the corresponding measurement with the UFTI photometry is outside the temperature range displayed here).

The photometric temperatures in Figure 4 are spread over a somewhat wider range of values than the spectroscopic temperature determinations. This can be explained by the fact that the photometric method is less accurate than the spectroscopic method in this particular range of effective temperatures. For instance, a difference of $\Delta T_{\text{eff}} = 2000$ K yields energy distributions (bottom of Fig. 1) that differ less than the predicted strengths of the Balmer line profiles for the same difference in T_{eff} .

Of greater interest in the context of our study is the comparison of photometric and spectroscopic effective temperatures for different versions of the mixing-length theory. This is shown in Figure 5 for the ML1, ML2, and ML3 parameterizations (in what follows we consider the UFTI and 2MASS infrared data as independent measurements and simply merge the samples). Although the spectroscopic T_{eff} values vary over a range of nearly 4000 K going from ML1 (less efficient version) to ML3 (more efficient version), the photometric temperatures remain nearly unchanged, as anticipated from our results shown in the top panel of Figure 1. Also, for both temperature estimates to agree, one must rely on a parametrization which is less efficient than the $ML2/\alpha = 1.0$ of the mixing-length theory (used to produce Fig. 5), in agreement with the lower value of $\alpha = 0.7$ adopted in the comparison shown in Figure 4, which is reproduced in Figure 6 by combining both UFTI and 2MASS data sets. These results add additional confidence to our conclusion that the atmospheric convective efficiency in DA white dwarfs is fairly well constrained and understood.

Despite these encouraging results, there are still some stars in Figure 6 for which the differences in photometric and spectroscopic temperatures are uncomfortably large. One example labelled A in the figure is G117-B15A. The spectroscopic solution yields $T_{\text{eff}} = 11,770$ K and $\log g = 8.04$ while the photometric solution with the UFTI infrared data is about 1250 K hotter. On the other hand, the photometric solution obtained with the 2MASS data is only

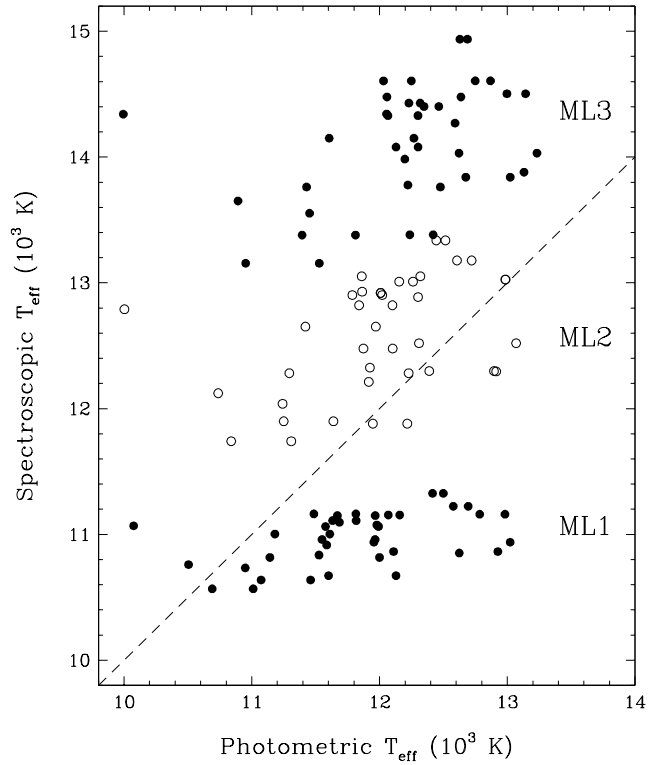


Figure 5. Comparison of photometric and spectroscopic effective temperatures for different versions of the mixing-length theory.

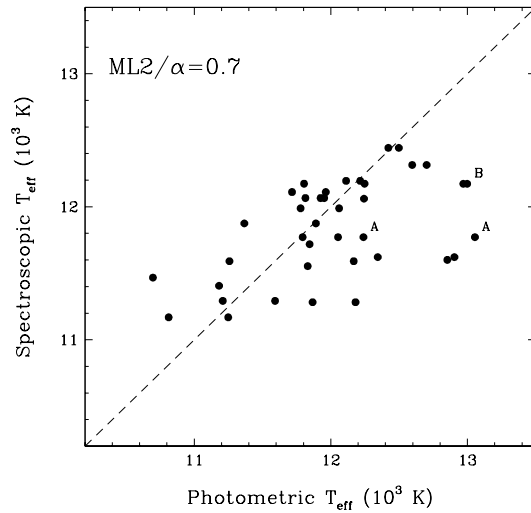


Figure 6. Comparison of photometric and spectroscopic effective temperatures obtained with model atmospheres calculated with $ML2/\alpha = 0.7$. A value of $\log g = 8.1$ was used for the photometric determinations. The objects labeled in the figure and discussed in the text correspond to (A) G117-B15A and (B) GD 165.

400 K hotter. We believe this reflects the difficulty with obtaining precise T_{eff} measurements for individual objects from photometry in this particular range of effective temperature due mostly to the sensitivity of the method, but also to problems with the calibration of the synthetic photometry. An alternative, perhaps more exotic explanation is provided by the second object, GD 165, labelled B in Figure 6. For this star, the spectroscopic solution yields $T_{\text{eff}} = 12,170$ K and $\log g = 8.13$. In this case, however, both solutions with the UFTI and 2MASS photometry agree within 90 K, with an average value of $T_{\text{eff}} = 12,950$ K, which is nearly 800 K hotter than the spectroscopic solution. Interestingly enough, had we used the $\text{ML2}/\alpha = 1.0$ version of the mixing-length theory, both spectroscopic and photometric temperatures would have been in perfect agreement (the spectroscopic temperature increases to a value of $T_{\text{eff}} = 13,030$ K in this case). Since GD 165 is one of the hottest ZZ Ceti star, perhaps our results is suggesting that convective energy transport is more efficient near the blue edge of the ZZ Ceti instability strip.

5. Conclusion

We have successfully demonstrated that energy distributions of ZZ Ceti stars built from optical *VRI* and infrared *JHK* photometric data provide a parameter-free and independent temperature scale for these stars that does not depend on the assumed value of $\log g$ or convective efficiency. Although we believe that the effective temperatures measured from photometry are less accurate for *individual* objects than temperatures obtained from the standard spectroscopic technique, our results nevertheless show that a parameterization of the mixing-length theory with $\text{ML2}/\alpha = 0.7$ provides, on average, an excellent internal consistency between photometric and spectroscopic temperatures. In particular, both methods yield consistent values for the boundaries of the ZZ Ceti instability strip between roughly $T_{\text{eff}} = 11,000$ K and 12,500 K.

Acknowledgments

This work was supported in part by the NSERC Canada and by the Fund FQRNT (Québec). P. Bergeron is a Cottrell Scholar of Research Corporation for Science Advancement. The United Kingdom Infrared Telescope is operated by the Joint Astronomy Centre on behalf of the Science and Technology Facilities Council of the U.K.

References

- Bergeron P, Ruiz M T, and Leggett S K 1997 *ApJ Suppl* **108** 339
- Bergeron P, Wesemael F, and Fontaine G 1992 *ApJ* **387**, 288
- Bergeron P, Wesemael F, Lamontagne R, Fontaine G, Saffer R A, and Allard N F 1995, *AJ* **449** 258
- Gianninas A, Bergeron P, and Fontaine G 2006 *AJ* **132** 831
- Holberg J B, and Bergeron P 2006 *AJ* **132** 1221
- Landolt A U 1992 *AJ* **104** 340
- Leggett S K et al. 2006 *MNRAS* **373** 781
- Lemke M 1997 *A&A Suppl* **122** 285
- Roche P F et al. 2003 *SPIE* **4841** 901
- Tokunaga A T, Simons D A, and Vacca W D 2002 *PASP* **114** 180